See discussions, stats, and author profiles for this publication at: https://www.researchgate.net/publication/234091898

Determination of distances between aluminum and spin-1/2 nuclei using cross polarization with very weak radio-frequency fields

ARTICLE in THE JOURNAL OF CHEMICAL PHYSIC	S · AUGUST 2002	
Impact Factor: 2.95 · DOI: 10.1063/1.1493196		
CITATIONS	READS	
15	15	

2 AUTHORS:



Gregor Mali

National Institute of Chemistry - Kemijski inš...

86 PUBLICATIONS 1,058 CITATIONS

SEE PROFILE



Venčeslav Kaučič

National Institute of Chemistry

90 PUBLICATIONS 959 CITATIONS

SEE PROFILE

Determination of distances between aluminum and spin-1/2 nuclei using cross polarization with very weak radio-frequency fields

Gregor Mali and Venčeslav Kaučič

National Institute of Chemistry, Hajdrihova 19, SI-1001 Ljubljana, Slovenia

Abstract

In this work the possibility of using cross-polarization (CP) experiment for the determination of distances between spin-5/2 and spin-1/2 nuclei in polycrystalline and amorphous materials was investigated. The properties of the method were experimentally studied in an isolated Al₂H spin system within the as-synthesized AlPO₄-31 and in "infinite" aluminophosphate networks within the calcined AlPO₄-31 and the hydrated VPI-5. In all three cases time-dependent oscillations due to coherent polarization transfer between aluminum and spin-1/2 nuclei were detected. The crucial parameters that influenced the visibility of dipolar oscillations were rotating-frame spin-lattice relaxation times of both nuclear species involved in a CP process and the homogeneity of rf fields. For a successful measurement the relaxation times, which varied remarkably with amplitudes of applied rf fields, had to be comparable to or larger than the period of time-domain oscillations. Rf-field inhomogeneity was minimized when amplitudes of rf fields were adjusted to the Hartmann-Hahn sideband matching condition $3\nu_{1I} + \nu_{1S} = \nu_R$, the nutation frequency of spin-5/2 nuclei was limited to $\nu_R/2 < 3\nu_{1I} < \nu_R$, and the nutation frequency of spin-1/2 nuclei was limited to $0 < \nu_{1S} < \nu_R/2$. Such adjustment assured also an efficient spin-locking of quadrupolar spins. Experiments in the as-synthesized and calcined AlPO₄-31 showed that in small isolated spin systems the time evolution of CP can elucidate the underlying geometry of the system whereas in "infinite" spin networks the splitting of a Pake-like doublet in the Fourier transform of a CP signal can yield an overall strength of the dipolar coupling. Although the use of weak rf fields reduced the robustness of the experiment it also introduced the selectivity of polarization transfer, which, as indicated by numerical simulation, in some cases allows the extraction of pair-wise dipolar couplings in multi-spin systems. The possibility of a selective polarization transfer and a selective determination of distances between octahedrally coordinated Al_1 nuclei and tetrahedrally coordinated P_2 and P_3 nuclei in the hydrated VPI-5 was demonstrated experimentally. 87.66.Uv, 33.40.+f

I. INTRODUCTION

Solid-state nuclear magnetic resonance (NMR) spectroscopy has become an indispensable tool for the investigation of polycrystalline and amorphous materials. An excellent example is a series of NMR studies in aluminophosphate molecular sieves, where magic angle spinning (MAS), multiple-quantum, and cross-polarization (CP) NMR investigations offer information about the number of magnetically inequivalent phosphorus and aluminum sites, about the coordination of these sites with framework oxygen atoms, hydroxyl groups, and water molecules, as well as about the connectivities among inequivalent aluminum and phosphorus sites. This qualitative information about the short-range order within molecular sieves is complemental to X-ray powder diffraction data and, indeed, helped to determine structures of a number of microporous aluminophosphates¹⁻⁴.

Recently, however, several mesoporous aluminophosphate molecular sieves were introduced, which do not possess a long-range order^{5–7}. Because NMR spectroscopy became a primary tool for the investigation of microscopic structures of these new materials, it should, possibly, provide not only qualitative information about connectivities but also quantitative information about internuclear distances. In rotating polycrystalline samples heteronuclear distances are most often measured by rotational echo double resonance (REDOR) method⁸ or one of its extensions^{9–12}. The original version of REDOR employs very strong π pulses synchronously with the sample rotation and in this way tries to re-introduce the heteronuclear dipolar coupling. The π pulses are assumed to be very short compared to the sample rotation period, which is hard to realize at high spinning frequencies. Nevertheless, REDOR functions quite well even under fast MAS conditions¹³. The method also proved to be highly robust and has been often successfully applied for measuring internuclear distances in singly or doubly labeled^{14–16}, and lately even in uniformly labeled biological solids^{17,18}.

Applications of REDOR to inorganic solids are less common^{19–21}, presumably because interactions within "infinite" inorganic networks necessarily involve multiple spins. A REDOR dephasing curve of a single multi-spin system exhibits long-term oscillations, which

depend on internuclear distances as well as on relative orientations of internuclear vectors, and might therefore be useful for identifying specific spin geometries. In a polycrystalline sample, however, the orientation-dependent oscillations are damped and only a smooth RE-DOR dephasing curve is usually observed. While in the limit of short evolution times the overall strength of the multi-spin dipolar coupling can still be extracted²², information about the underlying spin geometry is lost.

Recently, as an alternative to REDOR, CP²³ and Lee-Goldburg CP (LG-CP)²⁴ pulse sequences were employed for determining ¹⁹F²⁹Si and ¹H¹³C distances in zeolite octadecasil and in uniformly ¹³C-enriched tyrosine·HCl, respectively. The LG-CP technique performs better than the ordinary CP in the case of polarization transfer from or to abundant nuclei, because it substantially suppresses strong homonuclear couplings and thus prevents spin diffusion. In the absence of spin diffusion the time-domain signals of CP based pulse sequences build up in an oscillatory manner, which again reflects the geometry of the investigated spin system. As opposed to REDOR, however, CP and LG-CP methods are γ -encoded. This means that time-domain signals obtained by CP based techniques have a simpler angular dependence than those obtained by REDOR so that in powder samples the former should exhibit more pronounced long-term oscillations.

Promising CP experiments mentioned above suggest that they might be successfully used for measuring ²⁷Al⁻¹H and ²⁷Al⁻³¹P distances and for studying local geometry in microporous and mesoporous aluminophosphate molecular sieves. Unfortunately, a review of published material^{2,19,25} shows that in microporous aluminophosphates neither ²⁷Al⁻¹H nor ²⁷Al⁻³¹P CP measurements were thus far able to detect oscillations. There are, namely, some crucial differences between the CP measurement of ¹⁹F⁻²⁹Si distances, where oscillations due to coherent heteronuclear polarization transfer were detected, and the CP measurement of ²⁷Al⁻³¹P distances, where such oscillations were absent. Firstly, whereas ¹⁹F, ²⁹Si, and ³¹P are all spin-1/2 nuclei, ²⁷Al is a quadrupolar nucleus with spin 5/2. Aluminum spin-lattice relaxation time in rotating frame is, therefore, usually much shorter than corresponding relaxation times of fluorine, silicon, and phosphorus nuclei. In rotating samples strong

quadrupolar interaction becomes also time dependent and severely affects the spin-locking efficiency²⁶. Both, short rotating-frame spin-lattice relaxation time and time-dependent quadrupolar interaction, make an efficient spin locking of aluminum magnetization over a longer period of time very difficult. Secondly, ¹⁹F⁻²⁹Si spin pairs in octadecasil can very well be approximated by isolated spin pairs, whereas coupled ²⁷Al and ³¹P nuclei in aluminophosphates cannot. Each aluminum atom in a regular aluminophosphate molecular sieve is, namely, surrounded by four almost equally distant phosphorus atoms and *vice versa*. Destructive interferences of multi-spin interactions within this "infinite" network might as well be responsible for the suppression of long-term oscillations.

The objective of this work is to investigate the possibility of maintaining an efficient aluminum spin locking over the time, which corresponds to several periods of oscillations due to coherent heteronuclear ²⁷Al-¹H or ²⁷Al-³¹P polarization transfer, and the possibility of detecting these long-term oscillations by CP experiments. As it has just been discussed, in case of ²⁷Al-³¹P measurements the investigated spin system is very large, because each aluminum nucleus is surrounded by four phosphorus nuclei and each phosphorus nucleus is further surrounded by four aluminum nuclei etc. Very frequently, however, not all aluminum and phosphorus sites are crystallographically and magnetically equivalent. One can often encounter a situation, in which a particular aluminum crystallographic site is surrounded by four distinct phosphorus sites. An interesting question can then be raised, whether variablecontact-time CP experiments can measure individual ²⁷Al-³¹P distances, *i.e.* whether a multi-spin system of nuclei, which occupy inequivalent aluminum and phosphorus sites, can be decomposed into a set of ${}^{27}\mathrm{Al}{}^{-31}\mathrm{P}$ spin-pairs. We shall try to answer this question in the second part of this paper. Let us finally remark, that although the motivation for this investigation as well as examples within this work are all related to aluminophosphate molecular sieves, the discussed concepts and experiments are applicable to many other solid materials, in which distances among spin-1/2 and spin-5/2 nuclei are of interest.

II. THEORETICAL BACKGROUND

A detailed description of dynamics of polarization transfer between spin-1/2 and spin-3/2 nuclei was presented by Vega^{26,27}. In this section we shall only give a brief review with a minor extension to spin-5/2 nuclei. We shall begin with a description of an isolated I = 5/2, S = 1/2 spin pair under MAS conditions. The discussion will be limited to the cases where an amplitude of the applied rf field, ν_{1I} , is much smaller than the quadrupole frequency, $\nu_Q = 3e^2qQ/2I(2I-1)h$. In the doubly rotating frame, rotating at the frequencies of the two applied rf fields, the Hamiltonian can be written as

$$H = \tilde{\nu}_Q(t)(3I_z^2 - I(I+1)) - \nu_{1I}I_x - \nu_{1S}S_x + \tilde{\nu}_D(t)I_zS_z.$$
(1)

In an axially symmetric electric field gradient (EFG) the time-dependent quadrupole frequency is

$$\tilde{\nu}_Q(t) = \frac{1}{12}\nu_Q(3\cos^2\theta_Q(t) - 1) = \frac{1}{12}\nu_Q(G_1\cos(2\pi\nu_R t) + G_2\cos(4\pi\nu_R t)),\tag{2}$$

with

$$G_1 = \frac{3}{2}\sin 2\theta_m \sin 2\theta_Q', \ G_2 = -\frac{3}{2}\sin^2\theta_m \sin^2\theta_Q'.$$
 (3)

The polar angles $\theta_Q(t)$ and θ_Q' describe the orientation of EFG principal axes system within laboratory and MAS frames, respectively, θ_m is the magic angle, and ν_R is the frequency of sample rotation. In a similar way a time-dependent magnitude of the dipolar coupling can be expressed as

$$\tilde{\nu}_D(t) = \nu_D(G_1 \cos(2\pi\nu_R t) + G_2 \cos(4\pi\nu_R t)),\tag{4}$$

where the dipole frequency $\nu_D = \mu_0 \gamma_I \gamma_S \hbar / 8\pi^2 r_{IS}^3$. Of course, a different polar angle θ_D' enters the expressions for G_1 and G_2 .

Magic angle spinning causes $\tilde{\nu}_Q$ to oscillate between positive and negative values. This has a profound effect on the spin locking of I-spin central-transition coherence. The nature of

the spin locking is, namely, determined by the rate of the passages from positive to negative $\tilde{\nu}_Q^{26}$. The rate of the passages is described by the parameter

$$\alpha = \nu_{1I}^2 / \nu_Q \nu_R. \tag{5}$$

When $\alpha \gg 1$ the zero crossings are slow and described as adiabatic. In this limit the central-transition coherence is periodically demagnetized and remagnetized, giving rise to an echo-like time dependence of the spin-locking signal. When zero crossings are fast such that $\alpha \ll 1$, the passages are characterized as sudden, and do not affect the central-transition coherence. In the intermediate regime the spin-locking efficiency is greatly reduced.

For the description of the polarization transfer between spins I and S it is useful to express the Hamiltonian in Eq. (1) with fictious spin-1/2 operators²⁸ associated with the central (C_x, C_y, C_z) , the triple-quantum (T_x, T_y, T_z) , and the quintiple-quantum transitions (Q_x, Q_y, Q_z) , and with unit submatrices C_0 , T_0 , and Q_0^{27} . All these operators are listed explicitly in appendix A. Because any operator C_i commutes with any operator T_j and Q_j (i, j = x, y, z, 0), it is convenient to decompose the above Hamiltonian into three parts, H^C , H^T , and H^Q , which also commute with each other. In the limit of small rf fields we obtain

$$H = H^{C} + H^{T} + H^{Q}$$

$$= -8\tilde{\nu}_{Q}(t)C_{0} - 3\nu_{1I}C_{x} - \nu_{1S}C_{0}S_{x} + \tilde{\nu}_{D}(t)C_{z}S_{z}$$

$$-2\tilde{\nu}_{Q}(t)T_{0} - \nu_{1I}^{(3)}T_{x} - \nu_{1S}T_{0}S_{x} + \tilde{\nu}_{D}(t)T_{z}S_{z}$$

$$10\tilde{\nu}_{Q}(t)Q_{0} - \nu_{1I}^{(5)}Q_{x} - \nu_{1S}Q_{0}S_{x} + \tilde{\nu}_{D}(t)Q_{z}S_{z}.$$
(6)

The three parts of the Hamiltonian, corresponding to the central, the triple- and the quintiple-quantum transitions, have equivalent forms. However, whereas the nutation frequency of the central transition, $3\nu_{1I}$, is constant, the nutation frequencies for the triple- and quintiple-quantum transitions, $\nu_{1I}^{(3)} \propto \nu_{1I}^3/\tilde{\nu}_Q^2$ and $\nu_{1I}^{(5)} \propto \nu_{1I}^5/\tilde{\nu}_Q^4$, depend on the orientation of the EFG principal axes system. In a polycrystalline sample the last two nutation frequencies vary with orientation of the crystallites. Because of MAS the nutation frequencies also change with time, what means that the Hartmann-Hahn condition for CP between the

I-spin triple- or quintiple-quantum coherence and spins S cannot be established and that direct CP to or from triple- and quintiple-quantum coherence is not possible.

Let us now suppose that we excite quadrupolar nuclei with a selective $\pi/6$ pulse and thus prepare the initial state of the IS spin system, which can be described by a reduced density matrix of the form

$$\sigma(0) = C_x. \tag{7}$$

In the limit of the sudden-passage spin-locking regime the transitions between I-spin states are limited to the central manifold only. Since H^T , H^Q , and C_0 are inoperative as long as we stay within the central-transition subspace, the Hamiltonian that governs the evolution of the density matrix is simply

$$H' = -\tilde{\nu}_{1I}C_x - \nu_{1S}S_x + \tilde{\nu}_D(t)C_zS_z \tag{8}$$

and $\tilde{\nu}_{1I} = 3\nu_{1I}$. Apparently, within the limit $\nu_{1I} \lesssim \nu_R \ll \nu_Q$, which ensures $\alpha \ll 1$, the description of polarization transfer between the central transition of a quadrupolar nucleus and a spin-1/2 nucleus is equivalent to the description of polarization transfer between two spin-1/2 nuclei. Based on this analogy we can quickly write down two results. Firstly, the time dependence of the dipolar interaction due to fast MAS causes a familiar splitting of the Hartmann-Hahn matching condition into four sideband matching conditions:

$$\tilde{\nu}_{1I} \pm \nu_{1S} = 3\nu_{1I} \pm \nu_{1S} = n\nu_R,$$
(9)

with $n = \pm 1, \pm 2$. An efficient polarization transfer takes place only in a narrow band of rf fields around these conditions. The minus and plus sign in the matching conditions correspond to the zero- (flip-flop) and double-quantum (flip-flip) I-S transitions, respectively. Secondly, for an I = 5/2, S = 1/2 spin pair the variable contact time CP experiment at the n-th sideband yields the following S-spin signal²⁹

$$\langle S_x \rangle(t) = \operatorname{tr}(\sigma(t)S_x) = 1 - \cos(2\pi d_n t), \tag{10}$$

where

$$d_{\pm 1} = \frac{\sqrt{2}}{4} \nu_D \sin 2\theta_D' , \ d_{\pm 2} = \frac{1}{4} \nu_D \sin^2 \theta_D'. \tag{11}$$

The frequency of long-term oscillations, d_n , depends on |n|, on the polar angle θ'_D , and on the dipole frequency, ν_D , which is related to the I-S internuclear distance. In a polycrystalline sample the distribution of angles θ'_D spreads the frequencies d_n and thus attenuates long-term oscillations. The attenuation is, however, less pronounced as in the case of REDOR oscillations.

III. EXPERIMENTAL AND MATERIALS SECTION

Solid-state NMR experiments were performed using a 5 mm triple-tuned Doty CP MAS probehead on a narrow-bore Varian Unity Inova spectrometer operating at 156.35, 242.89, and 600.03 MHz for 27 Al, 31 P, and 1 H nuclei, respectively. Samples were typically spun with a spinning frequency of 10 kHz \pm 50 Hz. No spinning-speed controller was used to stabilize the spinning speed. More details about particular experiments are described in the next section.

²⁷Al⁻¹H CP MAS measurements were performed on an as-synthesized AlPO₄-31, and ²⁷Al⁻³¹P CP MAS experiments were carried out on a calcined AlPO₄-31 and a hydrated VPI-5 aluminophosphate molecular sieves. Fig. 1 schematically shows the three spin systems as well as corresponding MAS NMR spectra of aluminum and either hydrogen or phosphorus nuclei. In the as-synthesized AlPO₄-31 hydroxyl groups form Al–OH–Al bridges between some framework aluminum sites and thus give rise to 5-coordinated aluminum²⁵. Aluminum and hydrogen MAS spectra both show two main contributions. In the aluminum spectrum the contribution between 43 and 26 ppm belongs to 4-coordinated aluminum nuclei and the contribution between 17 and 2 ppm belongs to 5-coordinated nuclei. In the proton spectrum the resonances at 3.8 and 1.7 ppm are resolved. They belong to protons in the bridging hydroxyl groups and alkyl groups of the organic template molecules, respectively. A two-dimensional ²⁷Al⁻¹H CP MAS measurement showed that protons from the hydroxyl groups were efficiently cross-polarized from 5-coordinated aluminum nuclei but negligibly

from 4-coordinated nuclei²⁵, what indicates that protons from the organic molecules are far from 5-coordinated aluminum nuclei. Since in the as-synthesized AlPO₄-31 hydroxyl groups are relatively dilute, the Al–OH–Al bridges can very well be approximated by isolated Al₂H spin systems. The argument about dilute hydroxyl groups also suggests, that spin-diffusion among the protons under study is negligible so that ordinary CP pulse sequence can be used for a variable-contact-time experiment.

After the calcination, which removes the organic template from the pores of an aluminophosphate molecular sieve, the aluminum and phosphorus MAS NMR spectra of AlPO₄-31 both exhibit a single sharp resonance line. NMR spectra agree with the crystal structure, which was determined by the synchrotron powder diffraction³⁰ and which predicts only one aluminum and one phosphorus crystallographic site within an asymmetric unit of the calcined AlPO₄-31. The network of alternating aluminum and phosphorus nuclei can also be seen as a network of identical, but variously oriented AlP₄ groups, which are connected with each other through common phosphorus sites. The distances between an aluminum nucleus and four nearest phosphorus nuclei are similar, though not equal, and range from 0.303, 0.308, and 0.314 to 0.321 nm. They correspond to dipole frequencies of 455, 432, 408, and 382 Hz and are typical for aluminophosphate molecular sieves. The calcined AlPO₄-31 is a convenient probe material because of a very strong ²⁷Al-³¹P CP signal, which is due to narrow aluminum and phosphorus resonances, and because of short aluminum spin-lattice relaxation time, which enables fast repetition of experiments with the repetition delay of 0.1 s. Both properties affect the experimental time tremendously. Although phosphorus nuclei are abundant, spin diffusion among them is weak. The strength of the homonuclear coupling between nearest phosphorus nuclei, which are, for example, 0.45 nm apart, is only 216 Hz. For $^{27}\mathrm{Al}{^{-31}\mathrm{P}}$ CP measurements thus an ordinary pulse sequence can be used as well.

Contrary to the calcined AlPO₄-31, the hydrated VPI-5 has three inequivalent aluminum and three inequivalent phosphorus sites within the asymmetric unit³¹. Two aluminum sites, Al₂ and Al₃, are tetrahedrally coordinated by four framework oxygens. Their NMR resonances at about 42 ppm cannot be resolved one from another. The remaining aluminum site,

Al₁, is octahedrally coordinated by four framework oxygen atoms and two water molecules. Its NMR resonance at about -13 ppm is well separated from the resonances of thetrahedrally coordinated aluminum nuclei. Three completely resolved phosphorus signals at -33, -27, and -24 ppm can be assigned to nuclei, which occupy sites P_1 , P_2 , and P_3 , respectively³². The octahedrally coordinated aluminum nucleus Al₁ is in the first coordination sphere surrounded by four phosphorus nuclei occupying a P_3 , a P_2 and two P_1 sites. The hydrated VPI-5 aluminophosphate molecular sieve was used for studying the possibility of measuring individual Al_1-P_2 and Al_1-P_3 distances.

IV. RESULTS AND DISCUSSION

A. CP with very weak rf fields

The theoretical analysis of polarization transfer between quadrupolar and spin-1/2 nuclei shows that spin locking is efficient and CP process is relatively simple as long as we use low rf fields. In aluminophosphate samples rotating at 10 kHz we shall therefore limit to very weak rf fields on the aluminum channel so that ν_{1Al} will range from 0.5 to 9 kHz. First we will monitor $^{27}\text{Al}^{-1}\text{H}$ polarization transfer as a function of aluminum and proton nutation frequencies, and $^{27}\text{Al}^{-31}\text{P}$ polarization transfer as a function of aluminum and phosphorus nutation frequencies. By varying only one nutation frequency and keeping the other nutation frequency fixed one obtains a one-dimensional graph with four narrow "fingers" 33, which demonstrate that efficient polarization transfer occurs only around four sideband matching conditions. In two-dimensional graphs in Fig. 2, which show the variation of CP efficiency with both nutation frequencies, four "branches" instead of "fingers" can be seen. The stronger two "branches" correspond to $n=\pm 1$ sideband matching conditions and the weaker two to $n=\pm 2$ sideband matching conditions. In these experiments a constant contact time was chosen in such a way that maximal signal of $n=\pm 1$ sidebands was obtained. Since the amplitudes of $n=\pm 2$ sidebands rise slower with contact time than the amplitudes of

 $n=\pm 1$ sidebands (see Eq. (11)), at the employed contact times the former reach only a fraction of their maximal values. This is one of the reasons that in Fig. 2 the amplitudes of $n=\pm 2$ "branches" are lower than those of $n=\pm 1$ "branches".

Application of low rf fields allow us to observe not only zero- but also double-quantum transitions. The latter can be detected only in two "branches" with positive n provided that $3\nu_{1Al} < n\nu_R$. In all other cases the observed transitions are characterized as zero-quantum. Note that signals corresponding to zero- and double-quantum transitions have opposite sign. The zero-quantum transitions corresponding to the central matching condition (n = 0), although weak and invisible in Fig. 2, were observed as well.

If we vary aluminum nutation frequency and follow n=1 and n=-1 "branches", we can see that the efficiency of polarization transfer reaches its maximum already at $3\nu_{1Al} \approx 3$ kHz. Zero- and double-quantum polarization transfers are approximately equally efficient at that point. By further increasing the aluminum nutation frequency, the efficiency decreases in a nonuniform way. We can observe deep valleys, whenever aluminum nutation frequency approaches an integer multiple of the sample-rotation frequency, ν_R , and shallow valleys, whenever half-integer multiples of ν_R are approached. While the former were already detected and explained as a consequence of the second-order quadrupolar effects on spin locking of quadrupolar nuclei³⁴, the latter were not yet described. They might occur because of the crossing of the "branch" corresponding to zero-quantum transitions with the "branch" corresponding to double-quantum transitions. Since signals corresponding to zeroand double-quantum transitions have opposite sign, the observed shallow valleys in the efficiency curve could thus simply be due to a sum of positive and negative signals of unequal intensity. Following this hypothesis the valleys in the n = 1 and n = -1 "branches" at $3\nu_{1Al}=\nu_R/2$ could be due to the crossings with the n=0 and n=2 "branches", respectively, while the valley in the n=1 "branch" at $3\nu_{1Al}=3\nu_R/2$ could be due to the crossing with the n=2 "branch". There is only one more crossing of the "branch" corresponding to zero-quantum transitions with the "branch" corresponding to double-quantum transitions possible, namely, the crossing of the n=0 "branch" with the n=2 "branch". The crossing, however, takes place at $3\nu_{1Al} = \nu_R$ and thus overlaps with a deep valley.

The above described experiments confirm that for an efficient $^{27}\text{Al}^{-1}\text{H}$ or $^{27}\text{Al}^{-31}\text{P}$ polarization transfer it is advantageous to use very low rf fields on the aluminum channel, where very low means that aluminum nutation frequencies should obey the relation $3\nu_{1Al} < \nu_R$. An important question then follows, whether at such rf fields the rotating-frame spin-lattice relaxation times are sufficiently long to allow the observation of oscillations due to the coherent $^{27}\text{Al}^{-1}\text{H}$ or $^{27}\text{Al}^{-31}\text{P}$ polarization transfer. As we can see in Eq. (11) the largest possible frequency of oscillations in the case of a single spin pair is $\sqrt{2}\nu_D/4$. For an $^{27}\text{Al}^{-31}\text{P}$ spin pair within aluminophosphate molecular sieves, where a typical dipolar frequency is about 400 Hz, the frequency and the corresponding period of long-term oscillations are approximately 140 Hz and 7 ms, respectively. If we compare the period of oscillations with an aluminum rotating-frame spin-lattice relaxation time of about 0.4 ms, which was measured in VPI-5 under relatively slow MAS ($\nu_R \approx 3$ kHz) and high aluminum nutation frequency ($3\nu_{1Al} \approx 22$ kHz)¹⁹, we can immediately realize that under the described experimental conditions dipolar oscillations cannot be detected.

The rotating-frame spin-lattice relaxation measurements at low rf fields and fast sample spinning are more promising. Fig. 3 shows the variation of aluminum, proton, and phosphorus relaxation times with corresponding nutation frequencies. The slowest is the relaxation of phosphorus nuclei in the calcined AlPO₄-31. In the range of nutation frequencies between 2 and 25 kHz phosphorus rotating-frame relaxation time varies nonuniformly between 230 and 50 ms. Aluminum nuclei in the same sample relax uniformly and surprisingly slowly, with $T_{1\rho}^{Al}$ of about 20 ms, in the range of nutation frequencies between 2 and 18 kHz. Such relaxation times might be sufficiently long to allow the detection of oscillations due to ²⁷Al–³¹P polarization transfer. At higher aluminum nutation frequencies values of $T_{1\rho}^{Al}$ drop. For example, at the nutation frequency of 22 kHz the relaxation time is already 5 ms, which is still an order of magnitude larger than the relaxation time measured in VPI-5, but is probably to short to enable the measurement of ²⁷Al–³¹P distances.

The relaxation of aluminum nuclei in the as-synthesized AlPO₄-31 is faster. For nutation

frequencies between 2 and 17 kHz aluminum rotating-frame relaxation time varies between 7 and 13 ms. Whereas these values might be at the limit if we wanted to detect oscillations due to 27 Al $^{-31}$ P polarization transfer, they are probably sufficiently large to allow the observation of oscillations due to 27 Al $^{-1}$ H polarization transfer. The limiting factor in the detection of these oscillations might, however, be the relaxation of protons. Proton rotating-frame spinlattice relaxation times for the range of nutation frequencies between 2 and 15 kHz, namely, drop bellow 1 ms. The minimal value of 0.14 ms was measured at 8.5 kHz. If the nutation frequencies are increased above 15 kHz or decreased below 2 kHz the values of $T_{1\rho}^{H}$ begin to grow and at nutation frequencies of 36 kHz and 860 Hz reach values of 230 and 10 ms, respectively. As we shall see in the next section, proton relaxation has a great impact on the detection of long-term oscillations.

B. Variable-contact-time experiments

By carefully selecting rf fields on the aluminum, proton, and phosphorus channels we can indeed detect initial oscillations due to coherent 27 Al $^{-1}$ H and 27 Al $^{-31}$ P polarization transfer. Fig. 4 shows results of variable-contact-time CP experiments, which were carried out on the as-synthesized and calcined AlPO $_4$ -31. Time evolution of 27 Al $^{-1}$ H CP signals was monitored at n=-1 and n=-2 sideband matching conditions using aluminum nutation frequencies of 5.6 and 2.8 kHz, respectively. The sample was rotating with the frequency of 10 kHz. Obviously, proton rotating-frame spin-lattice relaxation times of about 2 and 20 ms at nutation frequencies of 15.6 and 22.8 kHz, respectively, were sufficiently long to allow the detection of oscillations over two periods. Time evolution of 27 Al $^{-31}$ P CP signals was monitored in a sample rotating at 15 kHz. Aluminum nutation frequency of 11.1 kHz and phosphorus nutation frequencies of 3.9 and 18.9 kHz were used. Although the monitored aluminophosphate spin network was practically "infinite", initial oscillations in the signal obtained by CP at the n=1 sideband condition were clearly detected. Because of multispin interactions, however, the oscillations decayed faster than those in the Al $^{-1}$ H CP signals.

Moreover, dipolar oscillations in the Al–P CP signal obtained at the n=2 sideband were almost completely damped. As we shall se later, this was not only because of multi-spin interactions but also because of rf-field inhomogeneity.

In the case of an isolated spin pair the dipole frequency characterizing the coupling of the two spins can be accurately determined by Fourier transformation of the time-domain signal³⁵. The Fourier transform exhibits a powder pattern similar to a Pake doublet. From the splitting of the doublet,

$$S_n = \nu_D / \sqrt{2}^{|n|},\tag{12}$$

which depends on the order of the sideband matching condition |n|, the dipole frequency can be extracted. In the case of multiple coupled spins the description is more complicated, because the time evolution depends on all dipole frequencies, which characterize pair-wise dipolar interactions, as well as on relative orientations of corresponding internuclear vectors. Recently, Ladizhansky and Vega³⁶ presented a theoretical description of CP in a multi-spin system composed of a single S = 1/2 spin and many I = 1/2 spins. They replaced the full time-dependent Hamiltonian by its zero order time-independent Hamiltonian in the interaction representation. The simplified Hamiltonian allowed efficient numerical simulations of CP in multi-spin systems. What is currently even more interesting for our discussion is that the simplified Hamiltonian enables also an analytical solution of a CP problem in a three-spin system. In this way at one of the sideband matching conditions the time-dependent I-S CP MAS signal for an I_2S system can be written as

$$\langle S_x \rangle (t) = 1 - \cos \left(2\pi t \sqrt{(d_n^{(1)})^2 + (d_n^{(2)})^2} \right).$$
 (13)

Here $d_n^{(1)}$ and $d_n^{(2)}$ characterize pair-wise $I^{(1)}-S$ and $I^{(2)}-S$ couplings, respectively (see Eq. (11)). By fitting the above expression to a measured signal and using $\nu_D^{(1)}$, $\nu_D^{(2)}$, $\theta_D^{(1)}$, and $\theta_D^{(2)}$ as variables of the fit, one can yield information about the geometry of the I_2S system.

Although the time evolution in Eq. (13) was calculated for a system of three spin-1/2 nuclei, we shall use it to approximately describe the time evolution of ²⁷Al-¹H CP signal

in the case of an Al₂H spin system. If we assume that the proton within such a system is approximately equally distant from both aluminum nuclei, we can set $d_n^{(1)} \approx d_n^{(2)}$. The frequency of oscillations in the CP signal is then $\sqrt{2}d_n^{(1)} \approx \sqrt{2}d_n^{(2)}$ and the corresponding splitting of the Pake-like doublet is

$$S_n \approx \nu_D^{(1)} / \sqrt{2}^{|n|-1} \approx \nu_D^{(2)} / \sqrt{2}^{|n|-1}.$$
 (14)

Experimentally determined splittings $S_{-1} = 1446$ Hz and $S_{-2} = 1036$ Hz indeed differ by a factor of $\sqrt{2}$ and thus agree with the above expression. The dipole frequency of a pairwise $^{27}\text{Al}^{-1}\text{H}$ coupling in the Al₂H system, obtained from these splittings, yields an $^{27}\text{Al}^{-1}\text{H}$ internuclear distance of about 0.28 nm. The distance is reasonable, but in the absence of crystallographic information about the position of protons we cannot verify it. Note that because the time-domain signals are rapidly decaying, sharp negative peaks centered at the zero frequency also appear in the Fourier transforms. However, if dipolar oscillations are pronounced, the central peaks don't disturb the splittings.

The analysis of ²⁷Al⁻³¹P CP in an "infinite" aluminophosphate network is more complicated. Although we realize that the splitting of the Pake-like doublet can depend on relative orientations as well as on the magnitude of the dipolar couplings, we shall suppose that the splitting provides an effective dipole frequency through a relation

$$S_n = \nu_D^{\text{eff}} / \sqrt{2}^{|n|}. \tag{15}$$

We can notice immediately that experimentally determined splittings $S_1 = 437$ Hz and $S_2 = 198$ Hz in this case don't differ by a factor of $\sqrt{2}$. The reason for this discrepancy is the fact that oscillations in the CP signal at the n=2 sideband condition are practically invisible, what means that the Pake-like doublet is severely disturbed by the central negative peak. The effective dipolar frequency obtained from the S_1 splitting is 618 Hz and is thus for a factor of 1.47 larger than the average of the pair-wise $^{27}\text{Al}^{-31}\text{P}$ dipolar frequencies, which is in the calcined AlPO₄-31 equal to 420 Hz. This result implies that in the network of alternating aluminum and phosphorus nuclei each aluminum nucleus is effectively coupled with approximately two phosphorus nuclei.

Experimental conditions that were used for the above described variable-contact-time experiments were a subject of a prior careful optimization. The influence of rotating-frame spin-lattice relaxation, sample rotation, and rf-field amplitudes on the visibility of oscillations is presented in Fig. 5. ²⁷Al⁻¹H polarization transfer was monitored at nutation frequencies, at which proton relaxation times were about 2, 0.5, and 0.2 ms. Whereas in the first case we can clearly detect oscillations over two complete periods, in the following two cases oscillations are attenuated and visible only over one period. Obviously, a rotating-frame spin-lattice relaxation time about as long as a period of dipolar oscillations is mandatory for the detection of oscillations. The frequency of the sample rotation has a great impact on the spin locking and therefore on the visibility of dipolar oscillations as well. As we can see in Fig. 5b ²⁷Al⁻³¹P polarization transfer in the sample spinning at 15 kHz gives slightly better results than in the sample spinning at 5 kHz. As opposed to REDOR, CP to or from quadrupolar nuclei thus prefers fast MAS.

Fig. 5c shows the time evolution of $^{27}\text{Al}{^{-31}}\text{P}$ CP signals recorded with phosphorus nutation frequencies of 1.1, 1.7, 4.4, and 7.2 kHz in a sample rotating at 10 kHz. Since phosphorus relaxation is slow and aluminum relaxation is relatively uniform over the region of applied rf fields, the effect of rotating-frame spin-lattice relaxation on the decay of dipolar oscillations can be neglected. Still we can clearly see that the oscillations are progressively attenuated with the increasing rf field on the phosphorus channel. The decay of time-domain oscillations corresponds to inhomogeneous broadening of a Pake-like doublet. Bertani and coworkers recently studied influence of the rf-field inhomogeneity on the Pake-like doublet, obtained by CP MAS in an isolated pair of spin-1/2 nuclei. They observed that the distribution of rf fields influences the intensity of the doublet and introduces inhomogeneous line broadening, whereas the splitting of the doublet remains unchanged. Describing the distribution of rf fields by a Gaussian shape with $\overline{\nu}_{1S}$ and σ_{1S} the mean value and standard deviation, respectively, the authors also showed that an accurate value of dipolar frequency can be obtained from the splitting of the doublet even if σ_{1S} is comparable to the width of the CP "finger".

However, inhomogeneous broadening is increasing with σ_{1S} and when dipolar oscillations are hardly detected and Pake-like doublets are not very pronounced it may prevent a correct determination of the splitting. In experiments with varying rf fields on the phosphorus channel, ν_{1P} , it is reasonable to expect, that the standard deviation σ_{1P} describing the distribution of rf fields increases with the mean rf field $\overline{\nu}_{1P}$. This does not necessarily imply that attenuation of dipolar oscillations in CP signals increases as well, because the width of the rf-field distribution at a given $\overline{\nu}_{1P}$ should be compared with the width of the CP "finger" at this $\overline{\nu}_{1P}$. In other words, one should consider a more appropriate measure describing the influence of inhomogeneous rf fields, that is the standard deviation of rf-field distribution divided by the width of the CP "finger". Fig. 6 shows that although the phosphorus nutation frequencies of 1.7 and 7.2 kHz differ by more than a factor of 4, the widths of the corresponding "fingers" are almost equal. If σ_{1P} approximately linearly depends on $\overline{\nu}_{1P}$, we can rightfully expect that attenuation of oscillations in Fig. 5c is due to the rf-field inhomogeneity that increases with phosphorus nutation frequencies.

Obviously, a proper selection of rf fields is very important for a successful measurement not only because of the rf-field dependent rotating-frame spin-lattice relaxation, but also because of the possibility to minimize effects of the rf-field inhomogeneity. We expected to observe similar effects in the case of variable aluminum nutation frequencies. The measurements, however, showed that as long as we were limited to aluminum nutation frequencies below ν_R rf field on the aluminum channel didn't play an important role. The results presented in Fig. 5c suggest that the optimal rf fields should be adjusted to the sideband matching condition $3\nu_{1I} + \nu_{1S} = \nu_R$ with $\nu_R/2 < 3\nu_{1I} < \nu_R$ and $0 < \nu_{1S} < \nu_R/2$. However, among the measurements of time-domain signals presented in Fig. 4 only the ²⁷Al-³¹P CP measurement at the n=1 sideband actually fulfilled the above requirements. When monitoring time evolution of polarization transfer at the n=2 sideband condition the applied rf fields were necessarily larger and the decay of dipolar oscillations was faster. In the case of ²⁷Al-¹H CP measurement the selection of rf fields was compromised between two requirements – the requirement for sufficiently long relaxation times and the requirement for low

rf-field inhomogeneity. If we wanted to detect oscillations we thus had to choose rf fields that were close to but not exactly within the above limitations.

C. Frequency offsets and selective CP

Application of weak rf fields in NMR spectroscopy is often unfavored because it can be accompanied with a pronounced sensitivity to frequency offsets and thus to experimental missettings. CP measurements with very small nutation frequencies are not an exception. Fig. 7 shows two effects of frequency offsets on $^{27}\text{Al}{}^{-31}\text{P}$ CP signals recorded at $\nu_{1P}=1.7$ kHz. Firstly, with an increasing offset of the carrier frequency on the phosphorus channel dipolar oscillations in time-domain signals become progressively attenuated. In the presence of an offset $\Delta\nu_{0P}$ the amplitude of an effective rf field in the rotating frame enlarges from $\nu_{1P}^{\text{eff}}=\nu_{1P}$ to

$$\nu_{1P}^{\text{eff}} = \sqrt{\nu_{1P}^2 + (\Delta \nu_{0P})^2}.$$
(16)

The mean effective rf field $\overline{\nu}_{1P}^{\text{eff}}$ of the rf-field distribution ceases to satisfy one of the sideband matching conditions so that the center of the rf-field distribution moves from the top of the "finger" towards its tail. The displacement affects time-domain CP signals in a similar way as the enlargement of the rf-field inhomogeneity. The increasing attenuation of dipolar oscillations with frequency offset was observed in case of very small aluminum and proton rf fields as well.

Secondly, in addition to oscillations due to coherent $^{27}\text{Al}^{-31}\text{P}$ polarization transfer also much faster, quite pronounced long-lasting oscillations can be observed in Fig. 7. Fourier transforms of time-domain signals show small, not well phased peaks at about $\pm \nu_{1P}$. We believ that the fast oscillations are periodic quasi-equilibria similar to those observed recently in CP MAS experiments on powder samples of ferrocene and alanine³⁷. The periodic quasi-equilibria were explained by considering the coupling of a spin system, described by a time-periodic Hamiltonian, to the lattice as a coherent broadening of the eigenvalues of the

Hamiltonian. They are expected to be physically observable in situations where relaxation is negligible compared to the coherent coupling of the spin system with the lattice³⁷.

Theoretical description of quasi-equilibria predicts oscillations with multiples of modulation frequency. Since in CP MAS experiments the Hamiltonian is modulated by sample spinning, the periodic quasi-equilibrium states are expected to be synchronized with spinning. Indeed, ¹H-¹³C CP MAS experiments in ferrocene and alanine detected oscillations with multiples of ν_R . The presence of oscillations with ν_{1P} in the case of $^{27}\mathrm{Al}^{-31}\mathrm{P}$ CP MAS experiment is therefore at first glance surprising. However, as we illustrate in appendix B the Hamiltonian in the interaction representation, describing polarization transfer between two spin-1/2 nuclei at the sideband condition $\nu_{1I} + \nu_{1S} = \nu_R$, is time modulated and the smallest among several modulation frequencies is ν_{1S} . This implies that oscillations with multiples of ν_{1P} in $^{27}\text{Al}^{-31}\text{P}$ CP MAS experiments are legitimate. As suggested above, periodic quasiequilibria in CP MAS experiments can be detected only when rotating-frame spin-lattice relaxation is sufficiently slow. Fast relaxation of aluminum and hydrogen nuclei is thus probably the reason that a similar effect as in the case of phosphorus frequency offsets was not observed also in the case of proton and aluminum frequency offsets. The rotating-frame relaxation times of phosphorus, aluminum, and hydrogen nuclei at nutation frequencies of about 2 kHz are, namely, 230 ms, 19 ms (calcined sample) or 7 ms (as-synthesized sample), and 3 ms, respectively. It thus seems that oscillations at ν_{1S} are exceptional rather than general, because there are two conditions which have to be fulfilled in order to detect oscillations – the nutation frequency ν_{1S} has to be small compared to ν_R and rotating-frame spin-lattice relaxation has to be very long.

Whereas an employment of small rf fields can reduce the robustness of CP experiments, it also introduces selectivity³⁸. The latter property might be particularly interesting in the cases when one would like to extract the strength of individual couplings in multi-spin systems. Let us consider a simple $IS^{(1)}S^{(2)}$ three-spin system. If resonances of spin $S^{(1)}$ and spin $S^{(2)}$ are resolved, one can investigate time evolution of $S^{(1)}$ -spin and $S^{(2)}$ -spin CP signals separately. Let us assume that the carrier frequency of the channel S is set to the

Larmor frequency of $S^{(1)}$ nuclei and that rf field is sufficiently strong that the frequency offset of the $S^{(2)}$ resonance can be neglected. By using the time-independent Hamiltonian³⁶ it is not difficult to describe a time-domain signal of spin $S^{(1)}$

$$\langle S_x^{(1)} \rangle(t) = \left(\frac{1 + \cos 2\varphi}{2} \right) \left(1 - \cos \left(2\pi t \sqrt{(d_n^{(1)})^2 + (d_n^{(2)})^2} \right) \right),\tag{17}$$

with $\varphi = \arctan(d_n^{(2)}/d_n^{(1)})$. The signal of spin $S^{(2)}$ can be obtained from the above expression by simply interchanging indexes 1 and 2. We can quickly realize that the $S^{(1)}$ -spin and $S^{(2)}$ -spin signals differ only in the first term which determines the signal amplitude, while the time evolutions of both signals are equal. This means that based on the frequency of dipolar oscillations we cannot determine individual $I-S^{(1)}$ and $I-S^{(2)}$ distances. However, if we lower rf fields on the channel S, sooner or later frequency offset will become important. Indeed, numerical simulation of CP in an $IS^{(1)}S^{(2)}$ spin system (Fig. 8) show that using rf fields that are in amplitude comparable to the offset of the $S^{(2)}$ resonance, the influence of spin $S^{(2)}$ on the signal of spin $S^{(1)}$ vanishes. The latter thus becomes equivalent to the signal of a CP measurement in a two-spin $IS^{(1)}$ system. Simulations were performed with a SIMPSON simulation package³⁹.

Numerical simulations indicated that CP experiments with very weak rf fields in particular cases enable a selective determination of distances in multi-spin systems. Particular cases are cases in which resonances of all spins of a multi-spin system are sufficiently separated that they can be selectively excited. In the case of an IS_n spin system this requirement is not so difficult to meet, since there is no restriction about the amplitude ν_{1I} other than that it must satisfy the relation $\nu_{1I} + \nu_{1S} = \nu_R$. Therefore almost arbitrary low amplitude ν_{1S} can be chosen to achieve a selective excitation. The general case of an I_mS_n spin system is more restrictive, because it can require that ν_{1I} and ν_{1S} have to be very small (comparable to the separation of corresponding resonances) at the same time. This can only be realized if ν_R is also very small, what however has drawbacks such as the appearance of numerous spinning sidebands and poor spin locking of quadrupolar spins.

We tried to demonstrate the potential of selective CP on a real system of the hydrated

VPI-5 aluminophosphate molecular sieve. We employed aluminum nutation frequency of 2.8 kHz and phosphorus nutation frequency of 7.2 kHz in a sample, which was rotating with 10 kHz. As we can see in Fig. 9 small aluminum nutation frequency enabled us to limit our investigation to only octahedrally coordinated aluminum nuclei occupying sites Al₁. Rf field on the phosphorus channel was larger from the rf field on the aluminum channel. Its carrier frequency was centered between phosphorus resonances assigned to nuclei P₂ and P₃. These two resonances were thus cross-polarized with approximately equal efficiencies, while the resonance of P₁ nuclei was about 2 kHz offset and thus cross-polarized substantially less efficiently. As expected the period of oscillations was now longer than the period of oscillations in the case of the calcined AlPO₄-31. This naturally made the oscillations more difficult to detect. Nevertheless, we can still see the initial part of oscillations in both, Al₁-P₂ and Al₁-P₃ variable-contact-time CP signals (Fig. 9). The oscillations are not very pronounced so that the splittings in their Fourier transforms do not offer a reliable information about dipolar frequencies. To extract the magnitude of Al₁-P₂ and Al₁-P₃ couplings we therefore fitted time-domain signals with a function²³

$$\langle S_x \rangle(t) = \left[\exp(-t/T_{1\rho}) - \exp(-k_1 t) g_n(t) \right] + \frac{N-1}{N+1} \left[\exp(-t/T_{1\rho}) - \exp(-k_2 t) \right].$$
 (18)

The expression describes the time evolution of the CP signal in a "real" isolated spin system which consists of a strongly coupled IS spin pair and N-1 weakly coupled (remote) I spins. $T_{1\rho}$ is the dominant relaxation time and k_1 and k_2 are first-order rate constants that describe the decay of transient oscillations and the spin diffusion with remote I spins. In the case of an ideal isolated spin pair (N=1) the second term in the above expression describing spin diffusion vanishes. The remaining part can be derived from Eq. (10) by including rotating-frame relaxation and performing powder averaging. The function $g_n(t)$ that describes the oscillatory behavior of S-spin polarization, namely, corresponds to $\cos(2\pi d_n t)$ averaged for a powder. The exact powder average can for the case of $n=\pm 1$ be expressed in terms of Bessel functions of the first kind as²³

$$g_{\pm 1}(t) = J_0 \left(\frac{\pi \nu_D t}{\sqrt{2}} \right) + 2 \sum_{k=1}^{\infty} \left[\frac{1}{1 - 4(2k)^2} J_{2k} \left(\frac{\pi \nu_D t}{\sqrt{2}} \right) \right]. \tag{19}$$

Expression in Eq. (18) together with the above $g_n(t)$ allows efficient nonlinear least-squares fitting of the experimental data.

Although we could not ensure a selective excitation of only one phosphorus resonance in our CP experiment in the hydrated VPI-5, Al_1 – P_2 and Al_1 – P_3 CP signals can still be very well described by expression in Eq. (18) what indicates that we monitored nearly isolated spin pairs. The dipolar frequencies obtained from fitting are in both cases 441 Hz \pm 22 Hz and correspond to Al_1 – P_2 and Al_1 – P_3 internuclear distances of 0.307 nm \pm 0.005 nm. This is reasonably close to 0.311 and 0.316 nm as determined, respectively, for Al_1 – P_2 and Al_1 – P_3 distances by the Rietveld refinement using X-ray powder diffraction data³¹. It seems that selective CP experiments could provide information about pair-wise couplings within multi-spin systems even in some real materials.

V. CONCLUSIONS

In this work we have shown that time-dependent oscillations due to coherent polarization transfer between spin-5/2 and spin-1/2 nuclei can be detected even in inorganic polycrystalline materials with "infinite" heteronuclear networks. Although the CP experiment itself is simple the employed rf fields have to be selected very carefully. The primary criterion for a successful detection of dipolar oscillations are sufficiently long rotating-frame spin-lattice relaxation times of both nuclear species involved in a CP process. Relaxation times, which can vary remarkably with amplitudes of applied rf fields, should be at least comparable to the period of time-domain oscillations. If compatible with rotating-frame relaxation rf fields should be adjusted to the Hartmann-Hahn sideband matching condition $3\nu_{1I} + \nu_{1S} = \nu_R$ with $\nu_R/2 < 3\nu_{1I} < \nu_R$ and $0 < \nu_{1S} < \nu_R/2$. The selection of very weak rf fields enables efficient spin-locking of quadrupolar nuclei and minimizes effects of rf-field inhomogeneity. Time evolution of CP in smaller spin systems (e. g. in isolated Al₂H groups) can provide

information about the underlying geometry of the system. In larger spin systems (e. g. in "infinite" network of alternating aluminum and phosphorus nuclei) the splitting of a Pakelike doublet in the Fourier transform of a CP signal can yield an overall strength of the dipolar coupling. Although CP at very weak rf fields is sensitive to frequency offsets, which can manifest in time-domain signals through attenuation of dipolar oscillations and through appearance of fast long-lasting oscillations associated with periodic quasi-equlibrium states, it is sometimes also desirable since it allows a selective determination of individual distances in multi-spin systems.

ACKNOWLEDGMENTS

We would like to thank Alenka Ristić and Nataša Novak Tušar for preparation of the samples. The Slovenian Ministry of Education, Science, and Sport is acknowledged for the financial support through research project Z1-3277.

APPENDIX A: FICTIOUS SPIN-1/2 OPERATORS

In this appendix fictious spin-1/2 operators that were used in the decomposition of the Hamiltonian in Eq. (6) are listed. If eigenstates of I_z are labeled by $|i\rangle$ with i=1,2,...6, the fictious spin-1/2 operators I_q^{ij} can be completely defined by listing all of their nonzero terms²⁸:

$$\langle i|I_x^{ij}|j\rangle = \langle j|I_x^{ij}|i\rangle = 1/2$$

$$\langle i|I_y^{ij}|j\rangle = -\langle j|I_y^{ij}|i\rangle = -i/2$$

$$\langle i|I_z^{ij}|i\rangle = -\langle j|I_z^{ij}|j\rangle = 1/2.$$
(A1)

Fictious spin-1/2 operators associated with the central, the triple, and the quintiple quantum transitions are then

$$C_q = I_q^{34}, \ T_q = I_q^{25}, \ \text{and} \ Q_q = I_q^{16},$$
 (A2)

where q=x,y,z. Unit submatrices are

$$C_0 = \delta_{33} + \delta_{44}$$

$$T_0 = \delta_{22} + \delta_{55}$$

$$Q_0 = \delta_{11} + \delta_{66}.$$
(A3)

It is now easy to derive following useful relations

$$I_z = 5Q_z + 3T_z + C_z \tag{A4}$$

$$3I_z^2 - I(I+1) = 10Q_0 - 2T_0 - 8C_0$$
(A5)

$$I_x = 3C_x + R_x, (A6)$$

where

$$R_{x} = \frac{1}{2} \begin{pmatrix} 0 & \sqrt{5} & 0 & 0 & 0 & 0 \\ \sqrt{5} & 0 & 2\sqrt{2} & 0 & 0 & 0 \\ 0 & 2\sqrt{2} & 0 & 0 & 0 & 0 \\ 0 & 0 & 0 & 0 & 2\sqrt{2} & 0 \\ 0 & 0 & 0 & 2\sqrt{2} & 0 & \sqrt{5} \\ 0 & 0 & 0 & 0 & \sqrt{5} & 0 \end{pmatrix}. \tag{A7}$$

The operator R_x is the "source" of operators T_x and Q_x in Eq. (6).

APPENDIX B: TIME MODULATION OF THE HAMILTONIAN IN THE INTERACTION REPRESENTATION

In this appendix we try to explain the presence of periodic quasi-equilibrium states, which can be detected as oscillations with frequency ν_{1S} in the I-S CP MAS signal. We shall limit to polarization transfer between two spin-1/2 nuclei at the sideband matching condition $\nu_{1I} + \nu_{1S} = \nu_R$ and shall allow frequency offset $\Delta\nu_{0S}$. We will show that the corresponding Hamiltonian in the interaction representation is time modulated also with frequency ν_{1S} .

The initial Hamiltonian describing an isolated pair of spin-1/2 nuclei is

$$H = -\nu_{1I}I_x - \nu_{1S}S_x + \nu_D(t)I_zS_z + \Delta\nu_{0S}S_z.$$
(B1)

In the doubly tilted frame, in which rf fields are pointing in the z direction, this Hamiltonian becomes

$$H = -\nu_{1I}I_z - \nu_{1S}S_z + \nu_D(t)I_xS_x - \Delta\nu_{0S}S_x$$

$$= -\frac{1}{2}(\nu_{1I} - \nu_{1S})(I_z - S_z) - \frac{1}{2}(\nu_{1I} + \nu_{1S})(I_z + S_z)$$

$$+ \frac{1}{4}\nu_D(t)(I^+S^- + I^-S^+ + I^+S^+ + I^-S^-) - \frac{1}{2}\Delta\nu_{0S}(S^+ + S^-).$$
(B2)

We can transform the Hamiltonian into an interaction frame by two successive transformations³⁶. The first one is defined by the operator

$$U^{(1)} = \exp(-i2\pi\nu_R(I_z + S_z)t/2)$$
(B3)

and transforms the Hamiltonian into a form with time-independent terms and terms oscillating with $\pm \nu_R/2$ and $\pm m\nu_R$ where m=1,2,3. Since we are interested in the time modulation with the lowest frequency we shall keep only time independent-terms and terms oscillating at half the frequency of the sample rotation. Furthermore, we shall assume that the rf fields match exactly the sideband condition $\nu_{1I} + \nu_{1S} = \nu_R$. The resulting Hamiltonian is then

$$H' = -\frac{1}{2}(\nu_{1I} - \nu_{1S})(I_z - S_z) + \frac{1}{8}\nu_D G_1(I^+S^+ + I^-S^-) -\frac{1}{2}\Delta\nu_{0S}(S^+ \exp(-i2\pi\nu_R t/2) + S^- \exp(i2\pi\nu_R t/2)).$$
 (B4)

The second transformation, defined by

$$U^{(2)} = \exp(-i2\pi(\nu_{1I} - \nu_{1S})(I_z - S_z)t/2), \tag{B5}$$

results in an effective Hamiltonian

$$H'' = \frac{1}{8}\nu_D G_1(I^+S^+ + I^-S^-) - \frac{1}{2}\Delta\nu_{0S}(S^+ \exp(-i2\pi\nu_{1S}t) + S^- \exp(i2\pi\nu_{1S}t)),$$
 (B6)

which is indeed time modulated with frequency ν_{1S} . According to the theoretical description of quasi-equilibria³⁷ oscillations with multiples of this frequency are expected in the I-S CP signal.

REFERENCES

- ¹ F. Taulelle, M. Pruski, J. P. Amoureux, D. Lang, A. Bailly, C. Huguenard, M. Haouas, C. Gerardine, T. Loiseau, and G. Ferey, J. Am. Chem. Soc. **121**, 12148 (1999).
- ² S. Caldarelli, A. Meden, and A. Tuel, J. Phys. Chem. B **103**, 5477 (1999).
- ³ A. Tuel, S. Caldarelli, A. Meden, L. B. McCusker, Ch. Baerlocher, A. Ristić, N. Rajić, G. Mali, and V. Kaučič, J. Phys. Chem. B **104**, 5697 (2000).
- ⁴ M. Roux, C. Marichal, J. L. Piallaud, C. Fernandez, Ch. Baerlocher, J. M. Chezeau, J. Phys. Chem. B **105**, 9083 (2001).
- ⁵ M. Schulz, M. Tiemann, M. Froba, and C. Jager, J. Phys. Chem. B **104**, 10473 (2000).
- ⁶ Y. Z. Khimyak and J. Klinowski, Phys. Chem. Chem. Phys. **3**, 616 (2001).
- ⁷ Y. Z. Khimyak and J. Klinowski, Phys. Chem. Chem. Phys. **3**, 2544 (2001).
- ⁸ T. Gullion and J. Schaefer, J. Magn. Reson. **81**, 196 (1989).
- ⁹ A. W. Hing, s. Vega, and J. Schaefer, J. Magn. Reson. **96**, 205 (1992).
- ¹⁰ T. Gullion, Chem. Phys. Lett. **246**, 325 (1995).
- ¹¹ T. Gullion and C. H. Pennington, Chem. Phys. Lett. **290**, 88 (1998).
- $^{12}\,\mathrm{J.}$ C. C. Chan and H. Eckert, J. Chem. Phys. $\mathbf{115},\,6095$ (2001).
- ¹³ C. P. Jaroniec, B. A. Tounge, C. M. Rienstra, J. Herzfeld, and R. G. Griffin, J. Magn. Reson. 146, 132 (2000).
- $^{14}\,\mathrm{A.~M.}$ Christensen and J. Schaefer, Biochemistry $\mathbf{32},\,2868$ (1993).
- ¹⁵ W. Hing, N. Tjabdra, P. F. Cottam, and J. Schaefer, Biochemistry **33**, 8651 (1994).
- ¹⁶ Y. Pan, N. S. Shenouda, G. E. Wilson, and J. Schaefer, J. Biol. Chem. **268**, 18692 (1993).
- 17 C. P. Jaroniec, B. A. Tounge, C. M. Rienstra, J. Herzfeld, and R. G. Griffin, J. Am. Chem.

- Soc. 121, 10237 (1999).
- ¹⁸ C. P. Jaroniec, B. A. Tounge, J. Herzfeld, and R. G. Griffin, J. Am. Chem. Soc. **123**, 3507 (2001).
- ¹⁹ C. A. Fyfe, K. T. Mueller, H. Grondey, and K. C. Wong-Moon, J. Phys. Chem. **97**, 13484 (1993).
- ²⁰ C. A. Fyfe and A. R. Lewis, J. Phys. Chem. B **104**, 48 (2000).
- ²¹ J. C. C. Chan and H. Eckert, J. Magn. Reson. **147**, 170 (2000).
- ²² M. Bertmer and H. Eckert, Solid State Nucl. Magn. Reson. **15**, 139 (1999).
- ²³ C. A. Fyfe, A. R. Lewis, and J. M. Chezeau, Can. J. Chem **77**, 1984 (1999).
- ²⁴ B. J. van Rossum, C. P. de Groot, V. Ladizhansky, S. Vega, and H. J. M. de Groot, J. Am. Chem. Soc. **122**, 3465 (2000).
- ²⁵ G. Mali, A. Meden, A. Ristić, N. Novak Tušar, and V. Kaučič, J. Phys. Chem. B 106, 63 (2002).
- $^{26}\,\mathrm{A.~J.~Vega,~J.~Magn.~Reson.}$ 96, 50 (1992).
- 27 A. J. Vega, Solid State Nucl. Magn. Reson. 1, 17 (1992).
- $^{28}\,\mathrm{S.}$ Vega, J. Chem. Phys. $\mathbf{68},\,5518$ (1978).
- $^{29}\,\mathrm{X}.$ Wu and K. W. Zilm, J. Magn. Reson. $\mathbf{104},\,154$ (1993).
- 30 J. M. Bennett and R. M. Kirchner, Zeolites ${\bf 12},\,338$ (1992).
- ³¹ L. B. McCusker, Ch. Baerlocher, E. Jahn, and M. Bülow, Zeolites **11**, 308 (1991).
- ³² G. Engelhardt and W. Veeman, J. Chem. Soc., Chem. Commun. 622 (1993).
- $^{33}\,\mathrm{M}.$ Sardashti and G. E. Maciel, J. Magn. Reson. **72**, 467 (1987).
- ³⁴ W. Sun, J. T. Stephen, L. D. Potter, and Y. Wu, J. Magn. Reson. A **116**, 181 (1995).

- ³⁵ P. Bertani, J. Raya, P. Reinheimer, R. Gougeon, L.Delmotte, and J. Hirschinger, Solid State Nucl. Magn. Reson. 13, 219 (1999).
- ³⁶ V. Ladizhansky and S. Vega, J. Chem. Phys. **112**, 7158 (2000).
- ³⁷ D. Sakellariou, P. Hodgkinson, S. Hediger, and L. Emsley, Chem. Phys. Lett. 308, 381 (1999).
- ³⁸ M. Baldus, A. T. Petkova, J. Herzfeld, R. G. Griffin, Mol. Phys. **95**, 1197 (1998).
- ³⁹ M. Bak, J. T. Rasmussen, and N. C. Nielsen, J. Magn. Reson. **147**, 296 (2000).

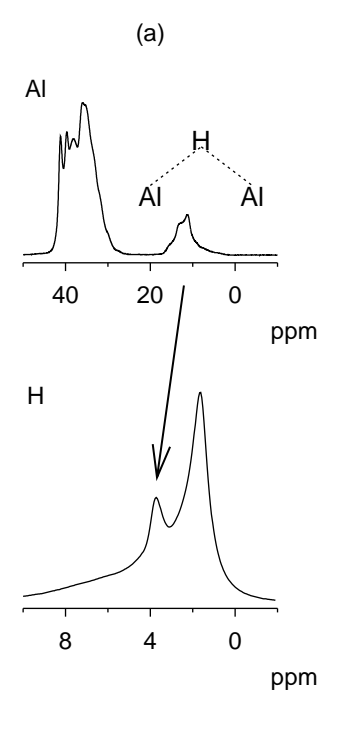
FIGURES

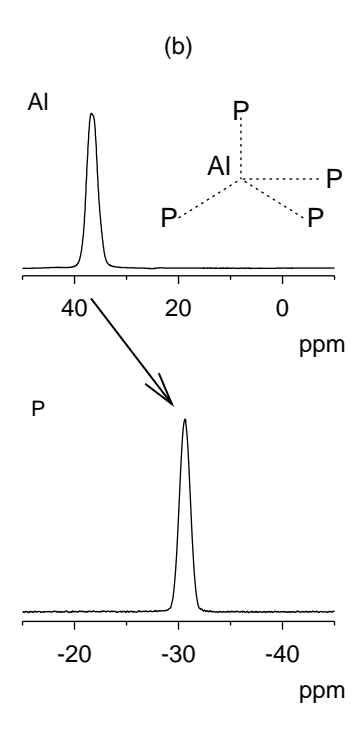
- FIG. 1. The spin systems which were studied in (a) as-synthesized AlPO₄-31, (b) calcined AlPO₄-31, and (c) hydrated VPI-5 aluminophosphate molecular sieves, as well as corresponding MAS NMR spectra of aluminum and either (a) hydrogen or (b,c) phosphorus nuclei. The dotted lines in schematically drawn spin systems show (a) Al–O–H and (b,c) Al–O–P connections. Aluminum spectra are referenced to 1 M solution of Al(NO₃)₃ in water, phosphorus to 85% H₃PO₄, and proton to tetramethylsilane. Arrows indicate among which resonances the polarization transfer was monitored.
- FIG. 2. Experimental $^{27}\text{Al}^{-1}\text{H}$ and $^{27}\text{Al}^{-31}\text{P}$ sideband matching at very low rf fields. (a) $^{27}\text{Al}^{-1}\text{H}$ CP with constant contact time of 0.5 ms and varying aluminum and proton nutation frequencies was carried out on the as-synthesized AlPO₄-31. (b) $^{27}\text{Al}^{-31}\text{P}$ CP with constant contact time of 2 ms and varying aluminum and phosphorus nutation frequencies was carried out on the calcined AlPO₄-31. In both experiments aluminum nutation frequency $(3\nu_{1Al})$ was varied between 1.5 and 27 kHz in 20 steps. Proton nutation frequency in (a) and phosphorus nutation frequency in (b) were varied in 100 steps between 0 and 37 kHz and between 0 and 27 kHz, respectively. (c) $^{27}\text{Al}^{-31}\text{P}$ CP efficiency along n = -1 (×) and n = 1 (+) "branches". The step in aluminum nutation frequency was a half of that in experiment (b). The solid line smoothly connects the measured points and should serve only as a guide for an eye.
- FIG. 3. Variation of rotating-frame spin-lattice relaxation times with corresponding nutation frequencies. Signs and + denote values of aluminum and proton relaxation times measured in the as-synthesized AlPO₄-31, whereas * and × denote aluminum and phosphorus relaxation times measured in the calcined AlPO₄-31. The dotted line smoothly connects the measured points and should serve only as a guide for an eye.

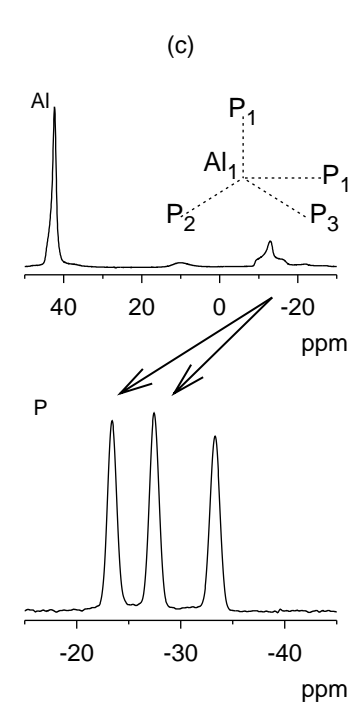
- FIG. 4. Variable-contact-time 27 Al $^{-1}$ H and 27 Al $^{-31}$ P CP experiments. (a) Time evolution of 27 Al $^{-1}$ H CP signal at the n=-1 (thick line) and n=-2 (thin line) sideband conditions in the as-synthesized AlPO₄-31 sample rotating at 10 kHz. The signals were recorded at $3\nu_{1Al}=5.6$ kHz, $\nu_{1H}=15.6$ kHz and $3\nu_{1Al}=2.8$ kHz, $\nu_{1H}=22.8$ kHz, respectively. (b) Time evolution of 27 Al $^{-31}$ P CP signal at the n=1 (thick line) and n=2 (thin line) sideband conditions in the calcined AlPO₄-31 sample rotating at 15 kHz. The signals were recorded at $3\nu_{1Al}=11.1$ kHz, $\nu_{1P}=3.9$ kHz and $3\nu_{1Al}=11.1$ kHz, $\nu_{1P}=18.9$ kHz, respectively. Fourier transforms of (a) and (b) after multiplication by -1 and baseline correction are presented in (c) and (d), respectively.
- FIG. 5. Visibility of oscillations in the variable-contact-time CP signals. (a) Influence of the proton rotating-frame spin-lattice relaxation times on the oscillations due to 27 Al $^{-1}$ H polarization transfer. The signals plotted with the solid, dashed, and dotted lines were recorded with proton nutation frequencies of 15.6, 12.8, and 7.2 kHz, at which proton relaxation times were about 2, 0.5, and 0.2 ms, respectively. In all experiments the sample rotated at the frequency of 10 kHz. (b) Influence of the frequency of sample rotation on the oscillations due to 27 Al $^{-31}$ P polarization transfer. The signals plotted with the solid, dashed, and dotted lines were recorded at the n=1 sideband condition with the aluminum nutation frequency of 11.1, 8.3, and 4.2 kHz. The sample was rotating at 15, 10, and 5 kHz, respectively. (c) Influence of rf fields applied to the phosphorus channel. The 27 Al $^{-31}$ P CP signals from top to bottom were recorded with the aluminum nutation frequencies of 2.8, 5.6, 8.3, and 11.1 kHz and phosphorus nutation frequencies of 7.2, 4.4, 1.7, and 1.1 kHz, respectively. The sample was rotating at 10 kHz.
- FIG. 6. Absolute and relative width of the "finger" corresponding to the n=1 sideband condition for an efficient $^{27}\text{Al}{}^{-31}\text{P}$ CP. (a) The efficiency of $^{27}\text{Al}{}^{-31}\text{P}$ polarization transfer as a function of the mismatch frequency $3\nu_{1Al} + \nu_{1P} \nu_R$ was measured in the sample rotating at 10 kHz with fixed aluminum nutation frequencies of 2.8 (solid line) and 8.3 kHz (dashed line) and phosphorus nutation frequencies varying around 7.2 and 1.7 kHz, respectively. (b) Results of the same measurement as in (a) but presented as a function of the relative mismatch frequency $(3\nu_{1Al} + \nu_{1P} \nu_R)/(\nu_R 3\nu_{1Al})$.

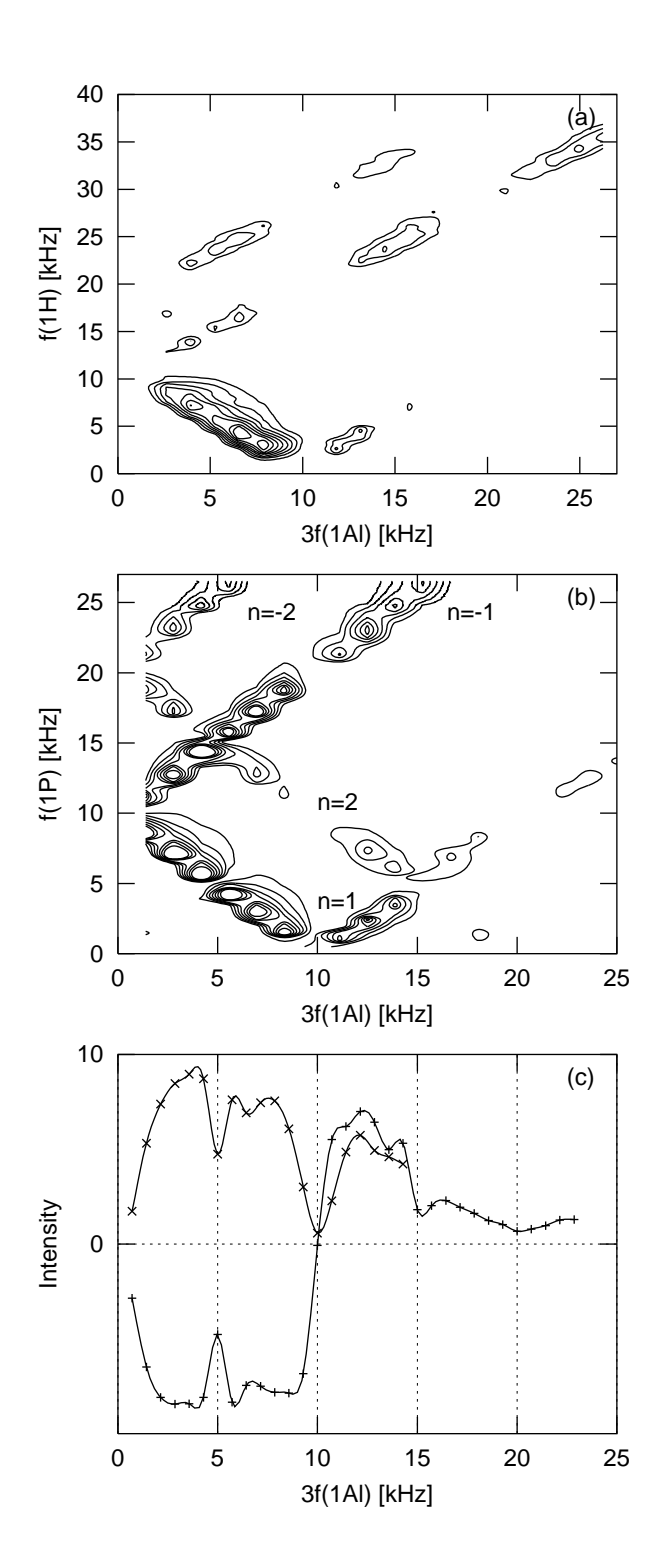
- FIG. 7. Influence of a frequency offset on $^{27}\text{Al}^{-31}\text{P}$ CP with very weak rf fields. (a) Variable-contact-time CP signals were recorded at $3\nu_{1Al}=8.3$ kHz and $\nu_{1P}=1.7$ kHz in a sample of calcined AlPO₄-31 rotating at 10 kHz. The carrier frequency of the phosphorus channel was set ± 500 Hz (thin lines) and ± 1000 Hz (thick lines) off the phosphorus resonance. (b) Fourier transforms of signals in (a).
- FIG. 8. Pake-like doublets of numerically simulated CP MAS measurements in an $IS^{(1)}S^{(2)}$ spin system. Dipolar frequencies of pair-wise $I-S^{(1)}$ and $I-S^{(2)}$ interactions were 400 and 450 Hz, while isotropic chemical shifts of spins $S^{(1)}$ and $S^{(2)}$ were 0 and 1000 Hz, respectively. Time-domain CP signals of $S^{(1)}$ spins were calculated in 200 points using time increment $\Delta t = 1/\nu_R = 100~\mu s$. Subsequently these signals were Fourier transformed to obtain Pake-like doublets. (a) Variation of Pake-like doublets with S-spin nutation frequencies ($\nu_{1S} = 9, 7, 5, 3, 1 \text{ kHz}$). Nutation frequencies of spins I were changed correspondingly to satisfy the relation $\nu_{1I} + \nu_{1S} = \nu_R$. (b) Comparison of numerically simulated Pake-like doublets corresponding to CP MAS measurements in an $IS^{(1)}$ two-spin system (thick line) and an $IS^{(1)}S^{(2)}$ three-spin system (thin line) calculated with $\nu_{1I} = 9$ kHz and $\nu_{1S} = 1 \text{ kHz}$. In a three-spin system again only the signal of spins $S^{(1)}$ was monitored.

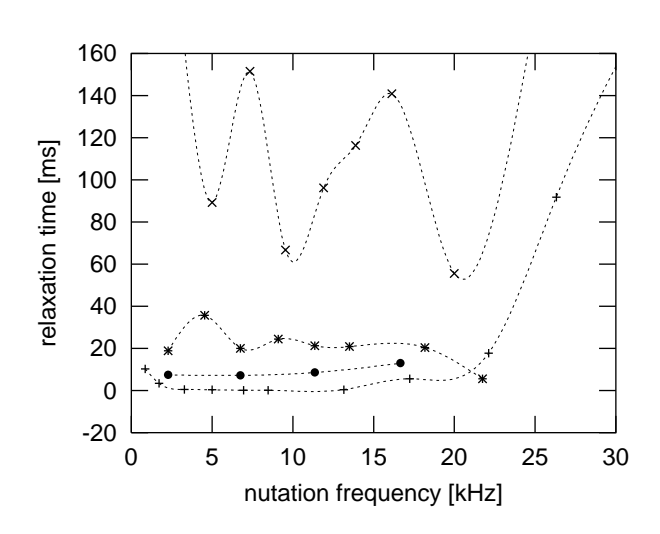
FIG. 9. Selective 27 Al $^{-31}$ P polarization transfer in the hydrated VPI-5 sample spinning at 10 kHz. Aluminum and phosphorus nutation frequencies were 2.8 and 7.2 kHz, respectively. The aluminum carrier frequency was set at the center of gravity of Al $_1$ resonance line and the phosphorus carrier frequency was centered between P $_2$ and P $_3$ resonance lines. Contact time was varied between 0 and 25 ms in steps of 0.5 ms. (a) Aluminum MAS spectrum (solid line) and offset dependent CP efficiency at $3\nu_{1Al} = 2.8$ kHz (dotted line). The latter was experimentally determined in the calcined AlPO $_4$ -31 by setting the phosphorus carrier frequency exactly on the phosphorus resonance while varying offset of the aluminum carrier frequency between -15 and 15 kHz in steps of 500 Hz. (b) Phosphorus MAS spectrum (solid line) and offset dependent CP efficiency at $\nu_{1P} = 7.2$ kHz (dotted line). The latter was experimentally determined in the calcined AlPO $_4$ -31 by setting the aluminum carrier frequency exactly on the aluminum resonance while varying offset of the phosphorus carrier frequency. (c) Al $_1$ -P $_2$ (×) and Al $_1$ -P $_3$ (+) variable-contact-time CP signals. Solid lines show fitted functions.

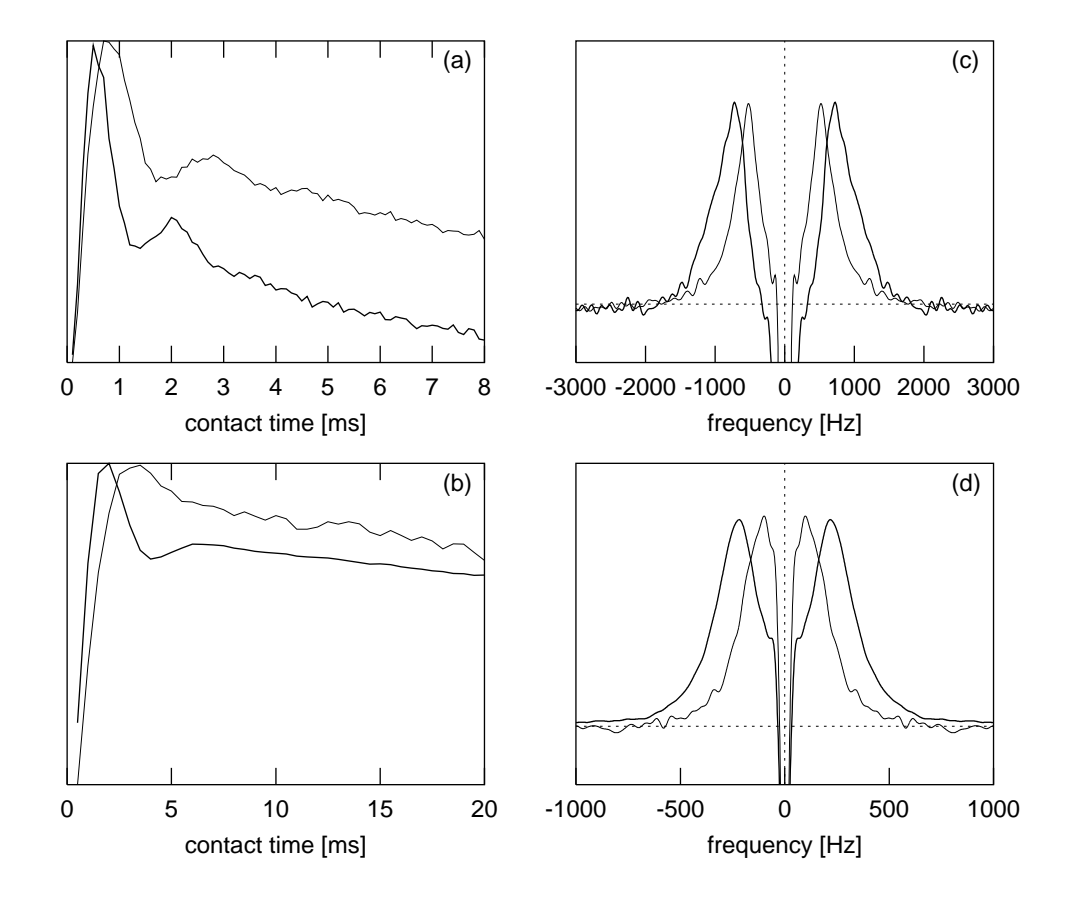


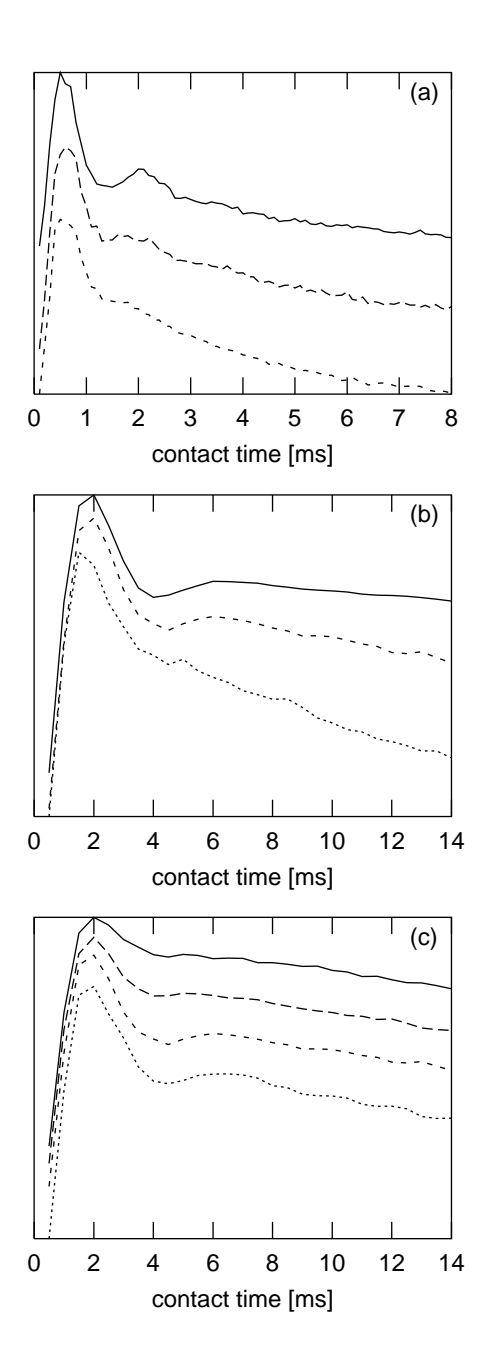


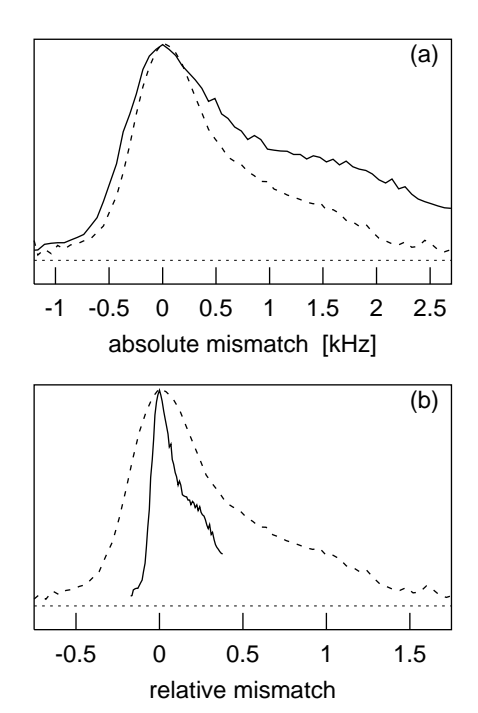


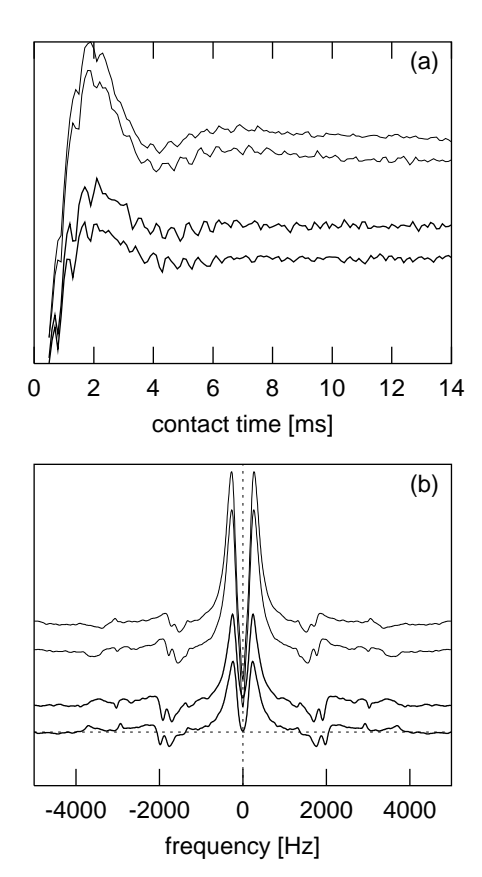


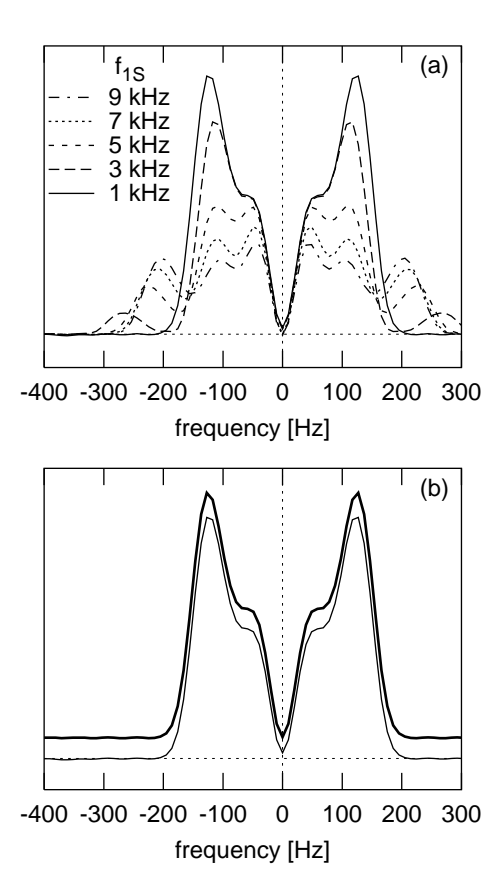


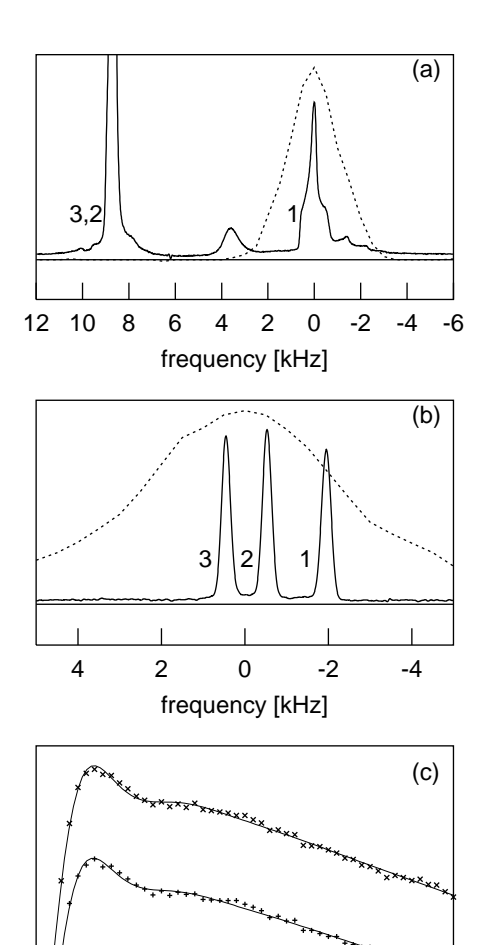












contact time [ms]